The ratio of the segmental to molecular friction coefficients is defined by eq 42; namely

$$\zeta/f = \frac{1}{3}\,\mathrm{Tr}\,(\mathbf{K}^{-1}) \tag{42}$$

with

$$\mathbf{K} = \sum_{i,j=1}^{x} \mathbf{Q}_{ij} \tag{34}$$

In the present case

$$\mathbf{K} = 2\lambda(1-\alpha)\mathbf{I} + 2(\mu(1-2\alpha) - \lambda(1-\alpha))\mathbf{nn} \tag{A1.14}$$

which, on substituting for λ and μ and using the axes $Ox_1x_2x_3$ defined, reduces to

$$\mathbf{K} = 2\ \mathrm{diag}\ (1/(1+2\alpha),\ 1/(1+\alpha),\ 1/(1+\alpha)) \tag{A1.15}$$

Whence

$$\mathbf{K}^{-1} = (1/2)\ \mathrm{diag}\ (1+2\alpha,\ 1+\alpha,\ 1+\alpha) \tag{A1.16}$$

and

$$(\zeta/f)_{\mathrm{Oseen}} = \frac{1}{2}(1 + 4\alpha/3) \tag{A1.17}$$

This is the result also given by the K-R approximation, eq 52.

Using the preaveraged Oseen tensor, one has

$$\mathbf{P}_{ij} = p_{ij}\mathbf{I} \tag{53}$$

with $p_{ij} = p_{ji}$ and, for the dipole

$$p_{11} = p_{22} = 1 \tag{A1.18a}$$

and

$$p_{12} = p_{21} = 4\alpha/3 \tag{A1.18b}$$

Equations 56 gives

$$\mathbf{Q}_{ij} = q_{ij}\mathbf{I} \tag{56}$$

and, here

$$q_{11} = q_{22} = \tau \tag{A1.19a}$$

$$q_{12} = q_{21} = -4\alpha\tau/3 \tag{A1.19b}$$

with

$$\tau = 1/(1 - 16\alpha^2/9) \tag{A1.20}$$

Use of eq 34 and 42 shows that

$$(\zeta/f)_{\mathrm{preav}} = \frac{1}{2}(1 + 4\alpha/3) \tag{A1.21}$$

Thus, as is known, for the special case of a dipole, the Oseen, K-R, and ⟨Oseen⟩ approximations give the same value of ζ/f.

References and Notes

(1) See: Stockmayer, W. H. In Les Houches Lectures 1973 "Molecular Fluids", eds. Balian, R., Weill, G. Eds.; Gordon and Breach: London, 1976.
(2) Kirkwood, J. G.; Riseman, J. *J. Chem. Phys.* **1948**, *16*, 565.
(3) Kirkwood, J. G. *J. Polym. Sci.* **1954**, *12*, 1.
(4) Mokrys, I. J.; Rigby, D.; Stepto, R. F. T. *Ber. Bunsenges Phys. Chem.* **1979**, *83*, 446.
(5) Edwards, C. J. C.; Rigby, D.; Stepto, R. F. T. *Macromolecules* **1981**, *14*, 1808.
(6) See: Burgers, J. M. *Proc. R. Acad. Sci. Amsterdam* **1938**, *16*, 113. ("Second Report on Viscosity and Plasticity", Chapter 3).
(7) ter Meer, H.-U.; Burchard, W.; Wunderlich, W. *Colloid Polym. Sci.* **1980**, *258*, 675.
(8) Burchard, W.; Schmidt, M. *Macromolecules* **1981**, *14*, 210.
(9) Zimm, B. H. *Macromolecules* **1980**, *13*, 592.
(10) Garcia de la Torre, J.; Jimenez, A.; Freire, J. J. *Macromolecules* **1982**, *15*, 148.
(11) Garcia de la Torre, J.; Freire, J. J. *Macromolecules* **1982**, *15*, 155.
(12) Rotne, J.; Prager, S. *J. Chem. Phys.* **1969**, *50*, 4381.
(13) Yamakawa, H. *J. Chem. Phys.* **1970**, *53*, 436.
(14) Fixman, M. *Macromolecules* **1981**, *14*, 1710.
(15) Silberszyč, W., private communication.
(16) Yamakawa, H. "Modern Theory of Polymer Solutions"; Harper and Row: New York, 1971.
(17) Lal, M.; Stepto, R. F. T. *J. Polym. Sci., Polym. Symp.* **1977**, *No. 61*, 401.
(18) Winnik, M. A.; Rigby, D.; Stepto, R. F. T.; Lemaire, B. *Macromolecules* **1980**, *13*, 699.
(19) Edwards, C. J. C.; Rigby, D.; Stepto, R. F. T.; Dodgson, K.; Semlyen, J. A. *Polymer* **1983**, *24*, 391.
(20) Flory, P. J. "Statistical Mechanics of Chain Molecules"; Interscience: London, 1969.
(21) Hill, J. L.; Stepto, R. F. T. *Trans. Faraday Soc.* **1971**, *67*, 3202.
(22) Varoqui, R.; Daune, M.; Freund, L. *J. Chim. Phys. Phys.-Chim. Biol.* **1961**, *58*, 394.
(23) Rigby, D. Ph.D. Thesis, University of Manchester, 1981.
(24) Zwanzig, R.; Keifer, J.; Weiss, G. H. *Proc. Natl. Acad. Sci. U.S.A.* **1968**, *60*, 381.
(25) Ullmann, R. *Macromolecules* **1974**, *7*, 300.

Self-Diffusion of Polystyrenes by Forced Rayleigh Scattering

Jeffrey A. Wesson,[1a] Icksam Noh,[1b] Toshiaki Kitano,[1c] and Hyuk Yu*

Department of Chemistry, University of Wisconsin, Madison, Wisconsin 53706.

Received August 9, 1983

ABSTRACT: The self-diffusion coefficients (D_s) of 4-(bromomethyl)azobenzene-labeled polystyrenes in tetrahydrofuran solution were measured for five molecular weights, from 32 000, to 360 000, in overlapping concentration ranges (in units of weight fraction) spanning from $c = 0.024$ g/g to $c = 0.648$ g/g. We have examined these measurements in the context of the Doi–Edwards theory, as extended by Graessley, and the de Gennes scaling theory. We found that for concentrations above c^*, the concentration for onset of semidilute behavior, the self-diffusion coefficient was well described by $D_s \propto M^{-2}$. On the other hand, the concentration dependence of D_s was neither described by a unique power law as in the de Gennes model nor directly proportional to $\eta_0^{-1}c^2$, where η_0 is the zero-shear viscosity of the solution, as predicted by Graessley using the Doi–Edwards model. Instead, we found the concentration dependence to be best described by Rouse theory, i.e., $D_s \propto \eta_0^{-1}c$. The absolute magnitudes of the diffusion coefficients agreed well with previous measurements by Lêger et al. (*Macromolecules* **1981**, *14*, 1732) for concentrations below 0.20 g/g, but there were substantial departures from their results at higher concentrations. The observed D_s values were found to be independent of label position and label concentration.

Introduction

W. H. Stockmayer's contributions to our present understanding of the chain dynamics of isolated macromolecules extends over 3 decades, and a tutorial on the subject marked by his usual incisive eloquence is given in Les Houches lectures.[2] The purpose here is to do our part, however small, in trying to extend the chain dynamics to concentrated solutions by examining chain self-diffusion

0024-9297/84/2217-0782$01.50/0

behaviors. The theoretical bases of polymer self-diffusion are afforded through the model of Doi and Edwards[3] and more qualitatively through the scaling arguments developed by de Gennes,[4,5] both based on his reptation model.[6]

In the case of the Doi–Edwards theory, the long-range configurational rearrangements, affecting the linear viscoelastic properties of fully entangled systems in bulk polymers or in concentrated solutions, are caused by reptation of a given polymer chain along its contour direction within a "tube"; such a tube is delineated by the surrounding topological constraints imposed by the chain entanglements. Thus, a variety of the phenomenological observables is shown to depend on the self-diffusion coefficient. As pointed out by Graessley,[7] the Doi–Edwards theory predicts the two important microscopic variables in terms of phenomenological quantities in addition to the tube diameter. They are the self-diffusion coefficient D_s and the slowest relaxation time called the tube disengagement time τ_d. In particular, the self-diffusion coefficient is given by

$$D_s = \frac{G_N^\circ}{135}\left(\frac{cRT}{G_N^\circ}\right)^2\left(\frac{\langle R^2\rangle}{M}\right)\frac{M_c}{M^2\eta_0(M_c)} \qquad (1)$$

where G_N° is the plateau modulus,[8] c is the mass concentration, $\langle R^2\rangle$ is the mean square end-to-end distance of a polymer chain, M_c is the entanglement coupling molecular weight of the polymer,[8] $\eta_0(M_c)$ is the limiting steady-shear viscosity at M_c, and RT has the usual meaning. According to eq 1, D_s is proportional to M^{-2} in the bulk state and in concentrated solution, where $\langle R^2\rangle$ still goes as M and G_N° is independent of M.[8] A similar M dependence of D_s is predicted by de Gennes[4,5] using scaling arguments. The concentration dependence of D_s is, however, not so well defined by eq 1 since G_N° depends on c by a square power while $\eta_0(M_c)$ depends on c by a progressively increasing power,[8] i.e., $\eta_0(M_c) \propto c^2 \sim c^6$. Hence, D_s depends on c through $\eta_0(M_c)$, which has no simple power dependence on c. The scaling prediction, on the other hand, sets the D_s dependence on c to be -1.75 in a good solvent and -3 in a Θ-solvent in the scaling regime of appropriate concentrations.

On the experimental side, there exist several approaches. In the macroscopic approaches, Beuche[9] had earlier used the radioactive tracer technique, and more recently, methods were devised for monitoring the boundary spreading of a concentration gradient of isotopically labeled chains in an otherwise identical pair of polymer samples. Klein[10] and Klein and Briscoe[11] have used infrared densitometry to measure the spreading, while Bartels et al.[12] used a small-angle neutron scattering technique. In the microscopic approaches, there are four techniques that have been used in tests of these theories. One is the pulsed field gradient NMR technique developed by Stejskal and Tanner,[13] first used by Tanner.[14] The second is forced Rayleigh scattering used by Lêger et al.,[15] and the third is the quasi-elastic light scattering technique as used by Amis et al.[16] Lastly, fluorescence photobleaching recovery is used by Smith.[17]

The current status of empirical testing by these different approaches is as follows. Using macroscopic methods, Klein[10] and Klein and Briscoe[11] show $D_s \propto M^{-2}$ with broad molecular weight polyethylene in bulk, and Bartels et al.[12] find the same relationship with narrow-distribution hydrogenated or deuterated polybutadiene in bulk. Lastly, Kumagai et al.[18] find a power of -2.7 for tritium-labeled polystyrene in bulk by the radioactive tracer technique. Several measurements of the self-diffusion coefficient in bulk polymers have also been made with microscopic techniques. Tanner[14] finds the molecular weight exponent to be -1.7 with fractionated poly(dimethylsiloxane) using the NMR technique, while Kimmich and Bachus[19] and Fleischer[20] find a power of -2 for both polystyrene and polyethylene using the NMR technique in each case. Smith et al.[21] report a -1.7 power law with fractionated poly(propylene oxides) by fluorescence photobleaching recovery, and Antonietti et al.[22] find a power of -2.2 for narrow-distribution polystyrene by forced Rayleigh scattering. Unfortunately, comparisons of the absolute magnitudes from these experiments are difficult due to the disparate conditions and polymers used by various workers.

Turning to measurements on polymer solutions where both the concentration and molecular weight dependencies can be tested by microscopic techniques, a much smaller set of measurements have been performed. Lêger et al.[15] report $D_s \propto M^{-2}c^{-1.75}$ for anionically prepared dye labeled polystyrenes in benzene solution in the scaling region, and they find no significant deviations from the scaling theory predictions. Callaghan and Pinder[23] find $c^{-1.83}$ for polystyrene in carbon tetrachloride over a limited concentration region using the NMR technique. Amis and Han[24] using the quasi-elastic light scattering technique find $c^{-1.75}$ for a decade or less in concentration and M^{-2} for a limited range of molecular weight if $c^{-1.75}$ is assumed for polystyrenes in tetrahydrofuran. Finally, in the only reported Θ-solvent measurements, Amis et al.[25] find M^{-2} and c^{-3} for the concentration ranges measured for polystyrenes in cyclohexane at 35 °C, again using quasi-elastic light scattering. As for the absolute value of D_s at comparable concentrations, Callaghan and Pinder[23] find good agreement with Lêger et al.[15] in a limited test, while Amis and Han[24] find their D_s values to be about 1 order of magnitude below those of Lêger et al.[15] for polystyrenes in good solvents. However, at larger polymer concentrations, both Callaghan and Pinder[23] and Amis and Han[24] show the concentration dependence of D_s getting stronger as the concentration increases, and Amis et al.[25] find that their Θ-solvent measurements of D_s agree with their good solvent data at large polymer concentrations. As stated earlier, eq 1 does not predict a well-defined power law of concentration whereas the scaling argument gives rise to the power of -1.75 in good solvents and -3 in Θ-solvents within the applicable concentration region. Among various results listed above, Lêger et al.[15] and Amis and Han[24] address most specifically both the molecular weight and concentration dependencies with polystyrene over 1 decade and 2 decades in molecular weight range, respectively. From this brief listing of the results from different groups using different techniques, it is apparent that the self-diffusion coefficient of a linear polymer must be examined in detail relative to molecular weight and concentration, particularly the progression from semidilute to concentrated solution to bulk.

The experimental method of our choice is the same as that of Lêger et al.,[15] which is variously called forced Rayleight scattering (FRS)[15,26,27] or the holographic grating technique.[22,28] A brief discussion of the technique is given as follows. Using the interference fringes produced by crossed laser beams, a harmonic distribution of the two states of a photochrome, the shifted and unshifted, is generated with a certain spatial regularity due to the fringe spacing, which ranges from a few microns to 100 μm. Subsequent erasure of the grating arises from two sources; the shifted photochrome has a finite lifetime and hence returns to the initial unshifted state by intramolecular reconversion, and the two states of the photochrome are mixed by diffusion. If the first is slower compared to the

second mechanism of erasure, the time dependence of the grating disappearance should be a direct measure of the diffusion kinetics of the photochrome. Appearance and disappearance of such gratings are monitored by using a third laser beam which is diffracted by the gratings, and the diffraction intensity is monitored as a function of time. Thus, an appropriate photochrome attached to polymer chains should afford a means to measure the self-diffusion coefficient of the polymer chains. Hence the most difficult problem for this method is the preparation of appropriately labeled polymer samples. The photochromic label used by Lêger et al.[15], (1′-(4-iodobutyl)-3′,3′-dimethylindolino-6-nitrobenzospiropyran), while giving a rather large contrast appropriate for FRS measurements of this type due to its large photochromic shift, requires a UV laser for photochromic shifting, and its shifted state lifetime is only about 35 s. Since we have some experience with both the chemistry and the use in FRS measurements of azobenzene derivatives, we choose 4-(bromomethyl)azobenzene as our dye label, expecting a photochromic shifted state lifetime of several hours,[29] allowing us to measure D_s as small as 10^{-11}–10^{-12} cm^2/s. The use of a photobleachable label, which was recently demonstrated,[22,28,30] would extend the range to some practical limit of $D_s \sim 10^{-13}$ cm^2/s but is not necessary for our purposes.

In contrast, the NMR technique is limited by the spin–spin relaxation process to $D_s \geq 10^{-9}$ cm^2/s,[23] and therefore is not useful at higher polymer concentrations. In the quasi-elastic light scattering (QLS) experiments, the slow relaxation process observed in semidilute solutions has been ascribed to the self-diffusion of the polymer chains in these solutions,[16,24,25] but other reports cast doubt on this assignment, giving no alternative explanation for its origin.[30,31] Although QLS experiments have the potential advantage of sampling the shortest distance scale, defined by $\kappa = (4\pi n/\lambda_0) \sin(\theta/2)$, at this point they can only be considered a probe of some dynamic property of a polymer solution and hence not a definitive method to probe self-diffusion.

Our focus here is to examine the self-diffusion coefficient of dye-labeled polystyrene as a function of concentration and molecular weight more completely than what Lêger et al.[15] have done at larger polymer concentrations. In doing so, we hope to elucidate the polymer dynamics in this region as well as the applicable range for the scaling predictions for solutions in good solvents. In addition, we contrast the behavior of the self-diffusion coefficient in cyclohexane at 34.5 °C, a Θ-solvent,[32] for some of the same polymers with the behavior in a good solvent over a narrower concentration range.

Experimental Section

1. Polymer Synthesis and Labeling. All polystyrene samples used were prepared by standard anionic polymerization techniques under high vacuum in two sequences. One series was labeled on one end, and a second series was labeled on both ends or in the center. Both procedures are described below. The resulting polymers were characterized by size exclusion chromatography, commonly called gel permeation chromatography (GPC), using high-performance liquid chromatography equipment and 10^6-, 10^5-, 10^4-, and 10^3-Å μ-Styragel columns (Waters Associates, Milford, MA). Tetrahydrofuran (THF) was used as the eluant, and the system was calibrated with narrow dispersity polystyrene standards (Pressure Chemical Co., Pittsburgh, PA). The molecular weight assigned to each sample was the peak molecular weight observed by GPC. The dye content of each sample was determined spectrophotometrically on a Cary 118 spectrophotometer (Varian Associates, Palo Alto, CA). The characteristics of the samples are summarized in Table I.

(a) Single-End Labeling. Polystyrenes A, B, and C were prepared with *sec*-butyllithium as a monofunctional initiator.

Table I
Characteristics of Polystyrenes Used

sample	$M \times 10^{-3}$ [a]	label position	label content (labels/chain)
A	32	end	0.25
B	46	end	0.38
C	105	end	0.23
D	130	center	2.0
E[b]	130	ends	1.4
F[b]	360	center	1.0

[a] GPC peak molecular weight. [b] Each sample showed a very small low molecular weight shoulder peak in GPC, presumably due to the presence of some monofunctional initiator.

Styrene was polymerized at room temperature in benzene for about 24 h. Each sample was then divided approximately in half, with one portion terminated with methanol and the other portion saved for dye labeling. We found that using the 4-(bromomethyl)azobenzene to terminate the polystyryl anion directly always resulted in a side reaction, yielding a mixture of the dye-labeled polystyrene and a polystyrene fraction with twice the molecular weight and no dye attached. The relative quantities could be varied with different termination conditions, but the dimer fraction was always present. Having attributed the dimeric termination to the metal–halogen exchange reaction as in polystyryllithium with benzyl chloride,[33] we decided to moderate the reactivity of active chain ends by changing them from carbanions to oxyanions before the termination with 4-(bromomethyl)azobenzene. The procedure was first to replace half (by volume) of the polymerization solvent (benzene) with THF and next to add a 5-fold molar excess of ethylene oxide in cyclohexane (3/1 by volume), which was allowed to react with the polystyryllithium for about 3 min at −77 °C. Finally, a THF solution of 4-(bromomethyl)azobenzene was added to the solution at a 2-fold molar excess and allowed to react for about 20 h at room temperature and 1 h at 50 °C. The exchange reaction between the bromo dye and polymeric alkoxide lead to a methylazobenzene-labeled polystyrene molecule and lithium bromide in solution. All steps through termination were carried out under high vacuum. After termination, the seals were broken, and each polymer was purified by repeated precipitations from THF into methanol and dried under high vacuum. The resulting polymers were comparable in their molecular weight distributions to those of the Pressure Chemical standard polystyrenes as judged by GPC, and there was no detectable difference in GPC peaks between the molecular weights of labeled and unlabeled chains in each sample.

(b) Double-End and Center Labeling. Samples D, E, and F were prepared from the bifunctional initiator (2,4-hexadienyl)lithium according to the procedure reported by Morton et al.[34] and Rubio[35] with two goals in mind. We found that the dye labeling on higher molecular weights from the first series was insufficient for FRS measurements, and we wanted to test the dependence of these measurements on the position of the label in the polymer chain. Therefore, after polymerizing the styrene in benzene for 5 h at room temperature, we divided each sample in thirds. One fraction was terminated with methanol as above, and the second fraction was end labeled by a procedure similar to that given above except that a 180-fold excess of ethylene oxide was added and allowed to react for 11 h at −5 °C. At this point a gel had formed, and a 90-fold excess of the dye was added to react for 8 h at room temperature. These fractions were then treated in the same manner as the samples in the first series. These samples, however, showed a low molecular weight shoulder peak in the GPC trace, presumably due to a small fraction of initiator that terminated on one end before polymerization. The low molecular weight material was estimated to be less than 5% of each sample by weight. The third fraction was terminated with methanol, precipitated, and dried as above in preparation for labeling in the center of the polymer chains.

Center labeling was accomplished by hydroxylating[36] the remaining double bonds in the initiator segment,[34,35] converting the hydroxyls to alkoxides, and reacting the alkoxide groups with 4-(bromomethyl)azobenzene as in the previous termination steps. The hydroxylation step was carried out by dissolving the bi-

functionally grown polystyrenes in a THF/methanol/water mixture (83/11/6 by volume) and adding a 4-fold molar excess of osmium tetraoxide along with about a 300-fold molar excess of 4-methylmorpholine 4-oxide. This mixture was allowed to react for 25 h at 65 °C, after which the polymer was precipitated in excess methanol and dried under high vacuum. The hydroxylated polymers were then dissolved in THF and reacted with a Na/K amalgam for 3 h at 40 °C under high vacuum to convert the hydroxyl groups to alkoxide ions. The remaining amalgam was filtered away, and the polystyrene alkoxide was allowed to react with a 60-fold molar excess of 4-(bromomethyl)azobenzene for 14 h at 40 °C before the vacuum was removed. As previously, the polymers were purified by repeated precipitation from THF into methanol and dried under high vacuum. No detectable difference was observed in the molecular weights of the three different fractions by GPC.

Since a dual-detector GPC experiment (with a refractive index detector and a visible absorbance detector at λ = 430 nm) indicated that the center-labeling procedure was more effective on the low molecular weight shoulder peak (presumably having the initiator segment on one end of the chain), sample D was fractionated to remove the low molecular weight species. This was accomplished through phase separation by lowering the temperature of a cyclohexane solution of sample D. This procedure was repeated three times to remove any one-end-labeled polymer, although we believe that the small amount of low molecular weight material present would not make a detectable difference in our measurements.

(c) Synthesis of 4-(Bromomethyl)azobenzene. 4-Methylazobenzene. Following the procedure of Burns et al.,[37] 6.3 g (0.06 mol) of *p*-toluidine in 15 mL of absolute ethanol was mixed with 6.3 g (0.06 mol) of nitrosobenzene in 15 mL of glacial acetic acid and stirred for 3 h at 40–50 °C and overnight at room temperature. Dark crystals formed, settled out, and were filtered. They were washed with 1 N HCl, followed by washing with 1 N NaOH and with distilled water. Subsequently, they were dissolved in an equivolume mixture of absolute ethanol and 95% ethanol warmed to about 60 °C and recrystallized by cooling. These crystals were washed first with a 70–80% (by volume) ethanol solution and finally washed with a 30% ethanol solution. Collected crystals were dried under high vacuum overnight at room temperature. The yield was about 70%.

4-(Bromomethyl)azobenzene. We followed the procedure of Nanya.[38] The above compound (2.5 g (0.013 mol)) was placed in a 100-mL round-bottom flask with a reflux condenser, and 54 mL of carbon tetrachloride, 2.28 g of *N*-bromosuccinimide (NBS), and 0.043 g (1.39 mol %) of benzoyl peroxide were added in the same. The mixture was gently stirred to allow refluxing of CCl_4 at 80–85 °C under illumination of an ultraviolet lamp (Hanovia) for 2 h. The unreacted NBS at the conclusion was filtered out and a majority of the CCl_4 was distilled out of the filtrate at 82–90 °C. The remaining solution was cooled to crystallize the product, which was subsequently recrystallized from benzene. The yield was about 30%. Characterizations were performed by optical spectroscopy, NMR, and melting point (61–64 °C).

2. Sample Preparation for FRS. Solutions for FRS measurements were prepared gravimetrically in small sample vials, and after the samples were dissolved completely (usually after several days), the solutions were transferred with a disposable pipet to the FRS cells, which were immediately capped, cooled in a dry ice–2-propanol bath, and sealed. Some of the highest solution concentrations were prepared by controlled evaporation of a more dilute solution in the FRS cell, and then the cell was sealed. THF (Gold Label grade, Aldrich, Milwaukee, WI) was used as received after filtering through 0.2-μm poly(tetrafluoroethylene) filters (Schleicher & Schuell, Inc., Keene, NH). Benzene had been purified by distillation, and the cyclohexane was distilled over CaH_2 (Aldrich) before use. Dust was removed from the polymer samples by filtering dilute (approximately 1%) solutions in THF through 0.5-μm poly(tetrafluoroethylene) filters (Schleicher & Schuell), which were then precipitated with filtered methanol and dried under high vacuum before use. The FRS cells were Pyrex spectrophotometer cells (some made in-house and others from Precision Cells, Hicksville, NY) of 0.5-, 1-, or 2-mm path lengths with 6- or 8-mm-o.d. Pyrex tubing attached to allow for sealing the cells. Two special cells that were equipped with stopcocks were used for the cyclohexane solutions, and these cells, once filled, were maintained at 45 °C before FRS measurements were performed at 34.5 °C. The measurements of D_s in good solvents were done at ambient temperature (approximately 22 °C), but temperature control was required for the measurements in cyclohexane. This was accomplished with the sample cell holder described elsewhere,[30] which was controlled to within 0.2 °C at 34.5 °C. The dye-labeled polymers were not blended with unlabeled polymer due to the relatively small FRS signal afforded by our dye, except for a test of dye label concentration at one molecular weight and concentration.

3. FRS Measurements. We used two different optical configurations for generating and detecting the transient gratings. One was described in a previous work,[39] and the other is the arrangement used by Lêger et al.[15] While we found no difference in the diffusion coefficients determined for a solution in either geometry, as a practical matter, the arrangement used by Lêger et al.[15] was far superior for these measurements. For the experiments, where the dye concentration is low and the contrast between unshifted and shifted states at the probing or reading wavelength is small, longer path length cells must be used to obtain sufficient contrast to diffract a measurable amount of light. It is then imperative to bring the reading beam in at the Bragg angle relative to the thick grating to maximize the diffracted intensity. Hence, most of the data was collected with the configuration of Lêger et al.[15]

Working in either optical configuration, we followed the same established procedure to acquire our data.[30,39] The grating spacing, d, was calculated from

$$d = \lambda/(2 \sin (\theta/2)) \tag{2}$$

where λ is the wavelength of the grating generating (writing) beams and θ is the crossing angle between the writing beams, determined by measuring the spot separation at a known distance from the crossing point. For these measurements, the 488.0-nm line of an Ar ion laser, controlled at 40-mW output, was used to write the gratings, which were then read with a 5 mW He/Ne laser at 632.8 nm. The writing beams were pulsed with an electromechanical shutter, and typically at widths between 25 and 150 ms. We have separately confirmed that the diffracted intensity relaxation time was independent of pulse width. The transient signals were acquired, accumulated, and analyzed with the electronics described previously.[30,39] We used the model function

$$V(t) = (Ae^{-t/\tau} + B)^2 + C^2 \tag{3}$$

to fit our data, where $V(t)$ is the measured photomultiplier output voltage as a function of time t, τ is the characteristic time of the decay, A is the preexponential amplitude of the diffracted optical field, B is the coherent scattering background optical field, and C^2 is the background intensity due to incoherent scattering and stray light. The four parameters were determined by a nonlinear regression analysis, and the fit quality was evaluated by visual examination of the residuals plot. Fits yielding nonrandom residuals were rejected. A typical data set and fit from the good solvent measurements are shown in Figure 1, where the decay begins immediately after the writing beams are turned off. An example of Θ-solvent measurements is displayed in Figure 2, which is typical for all polymer concentrations, grating spacings, and corresponding time scales. We are unable to give a plausible origin for this slow growth of diffracted signal but simply note some of the significant characteristics of the FRS experiments in cyclohexane. The maximum diffracted intensity at any concentration is at least a factor of 10 larger in cyclohexane and is obtained with writing pulse widths of 3–40 ms, typically much shorter than for the good solvent measurements. The rise in the diffracted signal seems to change at the same rate as the relaxation process with changing polymer concentration or grating spacing, and the signal shape is roughly constant over the entire range of writing pulse energies that gave measurable signals. On the other hand, the dye label 4-(bromomethyl)azobenzene by itself in cyclohexane at 34.5 °C gives a normal FRS signal such as in Figure 1. Knowing that something unusual was taking place in the signal-generating portion of these FRS experiments, we have chosen to analyze only the longest time behaviors to extract the grating decay times τ. We have systematically started the analyses at about 40% of the

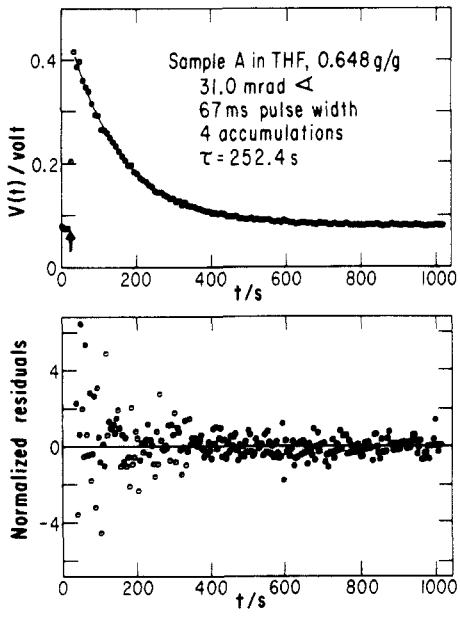

Figure 1. Rise and decay of the diffracted reading beam intensity. The top portion of this figure shows the average value of the photomultiplier output from four transients plotted as $V(t)$ in volts vs. time in seconds for a polystyrene in tetrahydrofuran using sample A, M = 32000, at c = 0.648 g/g. The background signal for a few pretrigger time intervals is included to emphasize the return of the signal to the base line. The shutter pulse position is indicated by the arrow, and the pulse width of 67 ms is less than the time interval between points of 4 s on this plot. The writing beam crossing angle of 31.0 mrad corresponds to a grating spacing d = 15.7 μm. The best fit curve to the decay profile using the model function as described in the text is drawn through the data in the upper graph, while the normalized residuals from that fit on the identical time scale are shown in the bottom graph, indicating a good fit to the data by their random distribution.

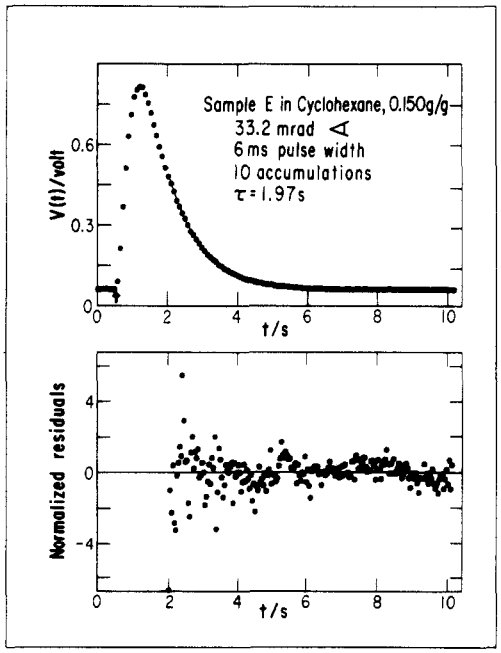

Figure 2. The same two plots as in Figure 1 for the average of 10 transients are shown for sample E, M = 130000, in cyclohexane at c = 0.150 g/g and d = 14.7 μm. The position of the shutter pulse is indicated as before, and the 6-ms pulse width is much less than the 400-ms time interval between points. The signal growth well after the writing pulse is clearly demonstrated; hence we fit only the long-time portion of the decay starting at about t = 2 s as shown by the fit curve and residuals plot.

maximum signal for each data set and found fits that lead to random residual plots.

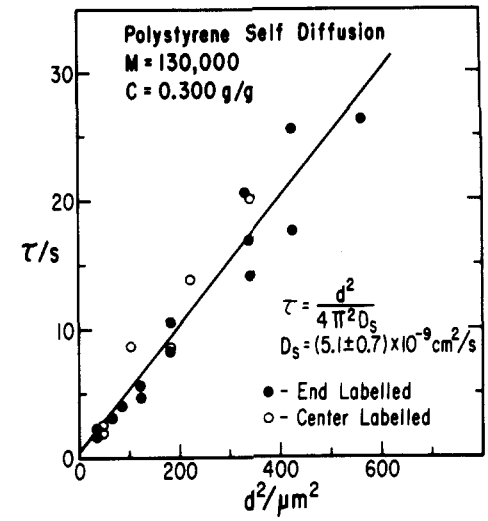

Figure 3. Linear plots of τ vs. d^2 for samples D and E, the M = 130000 polystyrenes, in tetrahydrofuran, both at c = 0.300 g/g. The least-squares fit line using all the data points yields D_s = (5.1 ± 0.7) × 10^{-9} cm^2/s at the 95% confidence limit. The filled circles represent the measurements on a solution of end-labeled polystyrenes, while the unfilled circles indicate the values found for the center-labeled polystyrenes of the same molecular weight at the same concentration. The agreement between these two data sets indicates that D_s is insensitive to the label position.

Having obtained the relaxation times at typically 10 different grating spacings for a particular sample, we made a plot of τ vs. d^2 as shown in Figure 3, and the diffusion coefficient was computed from the slope of the least-squares fit line through the data using the relation

$$\tau = d^2/4\pi^2 D_s \tag{4}$$

The least-squares analysis was executed without specifying the intercept as the origin, and the 95% confidence interval was calculated using the Student's t-distribution. The intercepts were found to be indistinguishable from the origin within the confidence limits and the uncertainties for the slopes were typically in the 10–20% range. The largest error bars were associated with the lowest concentrations at each molecular weight.

Results

D_s in THF and Benzene. Our results for the self-diffusion coefficient of polystyrene in THF and benzene are summarized in Table II and plotted in Figure 4 as log D_s vs. log c to facilitate comparisons with theoretical predictions. Also shown on the same graph as dashed lines are the data of Lêger et al.[15] for three of the molecular weights they studied, represented as accurately as we could read the data off their graph. In addition, the infinite-dilution diffusion coefficients for polystyrenes of the same molecular weights calculated with the data of Mandema and Zeldenrust[40] are plotted as additional reference points. Following the profile of D_s as a function of concentration for any of the molecular weights we studied, it is clear that slopes steeper than the −1.75 slope, predicted by scaling arguments and represented by the data of Lêger et al.,[15] are observed at polymer weight fractions greater than 0.2. In fact, at the highest concentrations studied for sample A, we find $D_s \propto c^{-13}$. We find it somewhat surprising that Lêger et al.[15] did not observe some departure from the −1.75 power law, especially for their 78300 molecular weight sample, since the concentration profile for our 46000 molecular weight sample (sample B) actually crosses through their data at a weight fraction of about 0.35. The difference in our observations cannot be attributed simply to the difference in solvents, benzene in their work and THF in ours; a measurement of D_s for sample C was carried out in benzene at a weight fraction of 0.404 (in-

Table II
List of Labeled Polystyrene Self-Diffusion in THF

sample	polymer wt fraction	$D_s \times 10^8$, cm²/s
A	0.223	13 ± 4
A	0.281	6.5 ± 1.5
A	0.403	1.7 ± 0.1
A	0.479	0.51 ± 0.02
A[a]	0.474	0.47 ± 0.06
A[b]	0.470	0.65 ± 0.15
A	0.584	0.071 ± 0.005
A	0.648	0.017 ± 0.001
B	0.048	75 ± 14
B	0.112	31 ± 13
B	0.200	12 ± 2
B	0.296	2.9 ± 0.2
B	0.378	1.4 ± 0.2
B	0.449	0.44 ± 0.02
B	0.544	0.064 ± 0.008
C	0.145	5.3 ± 2.8
C	0.250	2.5 ± 0.7
C	0.306	0.71 ± 0.14
C	0 369	0.41 ± 0.04
C	0.404[c]	0.21 ± 0.04
C	0.461	0.074 ± 0.006
D	0.024	57 ± 14
D	0.041	39 ± 12
E	0.070	15 ± 2
E	0.097	7.7 ± 0.7
E	0.152	3.2 ± 0.2
E	0.197	1.6 ± 0.2
E	0.258	1.0 ± 0.1
D, E	0.300	0.51 ± 0.07
F	0.161	0.33 ± 0.07
F	0.222	0.17 ± 0.05
F	0.283	0.062 ± 0.004
F	0.352	0.013 ± 0.003

[a] 1 part dye-labeled polystyrene blended with 3 parts unlabeled polystyrene of the same molecular weight; weight fraction represents total polymer content. [b] 1 part dye-labeled polystyrene blended with 7 parts unlabeled polystyrene of the same molecular weight; weight fraction represents total polymer content. [c] Solution prepared in benzene.

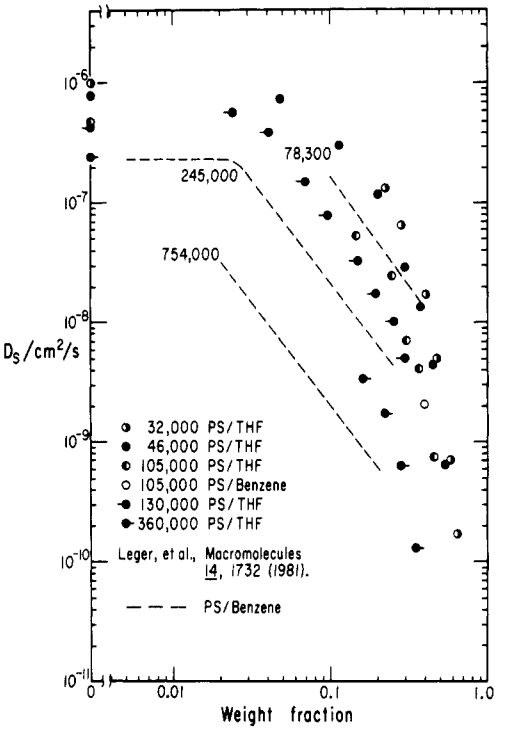

Figure 4. Plot of log D_s in cm²/s vs. log c in units of weight fraction (g/g). All of our measurements in good solvents collected in Table II are shown here, and they are compared with some representative portions of the concentration profiles for three molecular weights from Lêger et al.[15] for terminally (both ends) labeled polystyrenes by benzospiropyran in benzene solution. The predicted infinite-dilution diffusion coefficients for each molecular weight using the data of Mandema and Zeldenrust[40] are also indicated on the ordinate. The de Gennes prediction of $D_s \propto c^{-1.75}$ is represented by the data of Lêger et al.[15] at higher concentrations, but tracing the concentration profile for any of the samples we measured, it is obvious that slopes steeper than −1.75 are observed at higher polymer concentrations. This is shown to be independent of the two solvents used by the data point for $M = 105000$ at $c = 0.404$ g/g in benzene (unfilled circle) that blends smoothly with our THF data in the region where the slope is much steeper than −1.75. For $M = 32000$, where the largest concentrations are measured, the steepest slope of −13 is observed. Symbols for the various samples are identified on the plot, and the same symbol is used for samples D and E, which differ only in the position of the dye label, giving identical results for D_s as shown in Figure 3.

dicated on Figure 4 by a unfilled circle), and this point blends smoothly with our THF data for the same sample. This point falls well below where an extrapolation of the data by Lêger et al.[15] would place it. We also note that other workers found this type of deviation from good solvent scaling behavior at similar concentrations.[23,24]

At concentrations below 20%, we find our data to be in good agreement numerically with Lêger et al.[15] if the diffusion coefficients can be scaled by M^{-2}, which we will discuss further below. With our dye system we are unable to probe the transition region from dilute to semidilute solution very well, but our data are fully consistent with their earlier results at lower concentrations.

Extracting the molecular weight dependence of these self-diffusion data is a bit more difficult, since two of the molecular weights examined are too small to exhibit scaling behaviors before the concentration dependence of D_s begins to change rapidly at $c > 0.20$. Of course, within the context of the Doi–Edwards model, the M^{-2} exponent is only defined for fully entangled systems, which occurs at higher concentrations than required for scaling behavior. We test the predictions in two ways. If $D_s \propto M^{-2}$, the product M^2D_s should scale all of the data to a unique curve as a function of concentration. We illustrate this test in Figure 5A with a plot of log (M^2D_s) vs. log c. It can be seen that one smooth curve represents the entire data set quite well except for the lowest concentration of sample D and the two lowest concentrations of sample B. These points correspond to concentrations below c^*, the concentration for onset of semidilute behavior, in the scaling model, and the M^{-2} dependence is not expected in such a case. Alternatively, a smooth curve drawn through the concentration profile for one molecular weight in Figure 4 could be shifted vertically to correspond with the profiles for other molecular weights. These profiles should be parallel only over the regions of concentration where both molecular weights are above c^*. If the vertical shift factors are recorded for this curve-matching process and plotted against M on a double-logarithmic scale, the plot seen in Figure 5B is developed, using sample B as the reference concentration profile. Clearly, our data are well described by the M^{-2} power law for all concentrations greater than c^* when analyzed in either manner.

D_s in Cyclohexane. The self-diffusion coefficients observed in cyclohexane at 34.5 °C are summarized in Table III and shown graphically in Figure 6. To facilitate comparison with our good solvent data, M^{-2} scaling was applied to generate two more complete concentration profiles. Also, infinite-dilution diffusion coefficients in

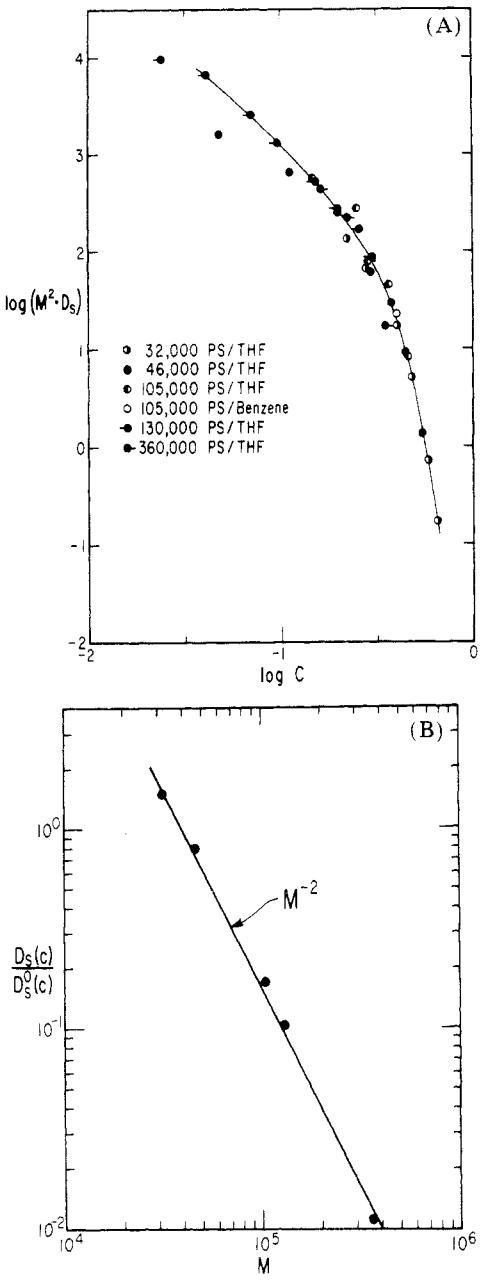

Figure 5. (A) Double-logarithmic plot of M^2D_s vs. c. All good solvent measurements are plotted in order to show the molecular weight dependence of D_s. A single smooth curve can be drawn as shown, in good agreement with all the data, except for the lowest concentration for M = 130 000 and the two lowest concentrations for M = 46 000, indicating that $D_s \propto M^{-2}$ is a good fit to our data. These three points correspond to solutions at concentrations below c^*, and M^{-2} scaling is not expected to hold in that region. The symbols for each sample are identified as in Figure 4. (B) Double-logarithmic plot of the vertical shift factor of the concentration profiles of $D_s(c)$ relative to the reference profile $D_s°(c)$ against M. The vertical shift factor $[D_s(c)/D_s°(c)]$ is calculated by drawing a smooth curve through the concentration profile of sample B, M = 46 000, as plotted in Figure 4, and shifting this curve vertically to best fit the profile at each of the other molecular weights while recording the shift factor. Sample B is assigned the value for $D_s(c)/D_s°(c)$ of 0.8. The line drawn represents the M^{-2} exponent predicted by the theories, and our data are consistent with such a prediction.

cyclohexane are calculated from the data of King et al.[41] for each molecular weight and plotted accordingly. The cyclohexane concentration profile at M = 130 000 appears to be merging with the good solvent data at the highest concentrations measured. Unfortunately, these solutions phase separate at higher dye-labeled polystyrene concentrations at 34.5 °C. Earlier experiments[25] suggested that these solutions should be stable at higher concentrations, but considering the poor solvent quality of cyclohexane, small perturbations, such as the presence of the dye moiety or a small amount of methanol carried in by incompletely dried polymer, might cause phase separation in these solutions. This aspect will be investigated further in the future. We are unable to draw any conclusions from the much more limited data set for M = 360 000, and there are not sufficient data to evaluate the molecular weight dependence at the Θ-condition.

Table III
Summary of Self-Diffusion Coefficients Measured in Cyclohexane at 34.5 °C

sample	wt fraction	$D_s \times 10^8$, cm²/s
E	0.028	15 ± 1
E	0.043	12 ± 1
E	0.074	7.9 ± 0.3
E	0.103	5.2 ± 0.3
E	0.150	2.9 ± 0.2
F	0.043	3.8 ± 0.8
F	0.060	2.4 ± 0.2

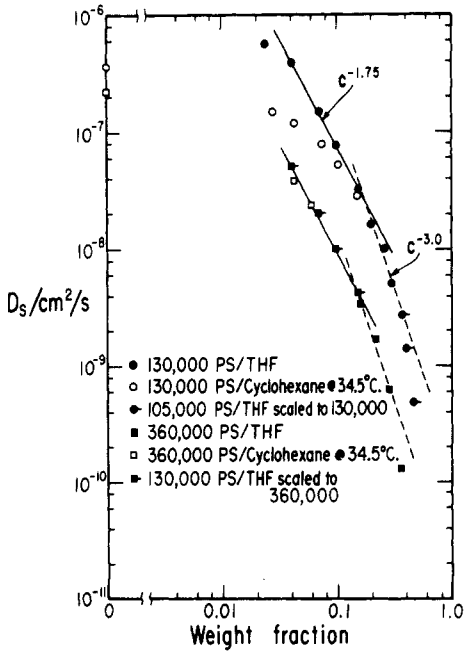

Figure 6. This plot of log D_s vs. log c shows the Θ-solvent measurements from Table III along with the good solvent measurements for the same samples. In addition, M^{-2} scaling is used to increase the concentration ranges spanned by good solvent measurements at each of the molecular weights as indicated, and infinite-dilution diffusion coefficients calculated from the data of King et al.[41] are also shown on the ordinate. The good solvent and Θ-solvent slopes predicted by de Gennes are drawn on the good solvent data for each molecular weight. It appears that the Θ-solvent data are merging smoothly with the good solvent data near the point where a −3 slope fits the good solvent data for M = 130 000, but no conclusions can be drawn for the M = 360 000 Θ-solvent data. The lines for −1.75 and −3.0 slopes on each good solvent profile intersect at about c = 0.17 g/g, and this can be considered the crossover from semidilute to concentrated solution and falls within the range predicted by Graessley.[43]

Photochromic Lifetime. Several potential complications are tested for this dye system to establish the limitations in our experiment. The shifted-state lifetime of the photochromic dye was determined by measuring the decay time for a portion of sample C evaporated to near bulk in a 0.5-mm path length cell. The shifted-state lifetime, τ_1, as determined by the procedure outlined above, is found to be about 500 s, when a 5-mW He/Ne laser is

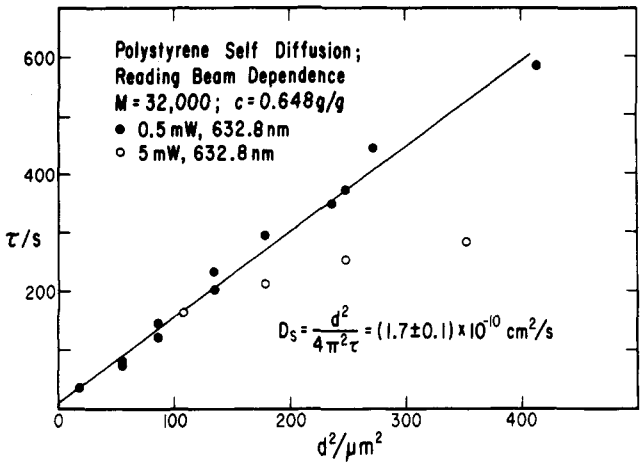

Figure 7. Plot of τ vs. d^2 illustrating the effect of the reading beam intensity on the measured lifetime. The filled circles correspond to a 0.5-mW reading beam, and the unfilled circles to the 5-mW reading beam. The line drawn is the least-squares fit to the filled circles only, and D_s is calculated from the slope to be $(1.7 \pm 0.1) \times 10^{-10}$ cm²/s, where the error range represents the 95% confidence interval. Clearly, for d^2 values greater than 150 μm², the observed τ with the 5-mW reading beam is substantially below that of the diffusion-controlled process represented by the filled circles. τ_1 calculated with eq 5 to analyze the 5-mW data plus the 0.5-mW data for d^2 values below 100 μm² is 420 ± 240 s at 95% confidence, in reasonable agreement with the directly measured τ_1 of 500 s.

used as the reading beam (our standard configuration). However, as shown in Figure 7, we find that reducing the reading beam intensity extends the dye lifetime dramatically, so clearly the He/Ne laser is causing some change in the lifetime of the shifted state. The analysis scheme proposed earlier[15] to deal with dye lifetime effects is as follows:

$$1/\tau_{app} = 1/\tau_1 + 4\pi^2 D_s/d^2 \quad (5)$$

where τ_{app} is the measured decay time. Equation 5 tends to give somewhat lower values of D_s than an analysis using the linear portion of the τ vs. d^2 plot. This test is performed on data as in Figure 7, where eq 5 is used to fit the 5-mW illumination data plus the lowest d^2 values of the 0.5-mW data and compared to the τ vs. d^2 analysis of the 0.5-mW data. The crucial point to be emphasized about fitting data with eq 5 is that the determination of the diffusion coefficient is most sensitively influenced by the lowest d^2 value measured; however, it may be the only way to treat some of the data. For example, the lowest concentration measured for sample F has to be treated in this manner, since the diffracted signal is too weak to allow reduction of the reading beam intensity.

Labeling Position and Concentration. Dye label position and dye label concentration are also tested. In Figure 3, the direct comparison of end- vs. center-labeled samples can be seen for samples D and E, both at 0.300 g/g, indicating no measurable influence of label position on the self-diffusion coefficient. Both of these samples are used in defining different points in the concentration profile for the 130 000 molecular weight polymer shown in Figure 4 and in Table II, and the smooth curve obtained is a further demonstration of the invariance of D_s with label position. The dye concentration dependence was tested for sample A at about 0.48 g/g. To do this, sample A was blended with unlabeled polystyrene of the same molecular weight at both 1/3 and 1/7 ratios of labeled to unlabeled polystyrene, and these mixtures were dissolved to approximately the same total polystyrene concentration as the all dye-labeled sample. All three diffusion coefficients are identical within the experimental uncertainty, as seen in Table II. While unblended sample A gives a D_s value of 5.1×10^{-9} cm²/s (±4%), those blended by 1/3 and 1/7 gave the values of 4.7×10^{-9} cm²/s (±13%) and 6.5×10^{-9} cm²/s (±23%), respectively. Thus there seems to be no particular trend in D_s values as we dilute the labeled with the unlabeled chains, except the uncertainty becomes greater. We do not, however, claim that these results should be taken as conclusive evidence for the invariance of D_s with label concentration. There may well be some label concentration dependence but it cannot be discerned with these samples within our present measurement precision. To this extent, we put forth our observed D_s values as the self-diffusion coefficients of polystyrenes and not just those of labeled polystyrenes. We finally note here that the mole fraction of the dye relative to the monomer concentration in these samples ranged from 7.8×10^{-4} to 1.1×10^{-4}.

Discussion

In comparing our work to predictions of the de Gennes scaling theory and the Doi–Edwards theory as extended by Graessley, we will first discuss the molecular weight dependence and then the concentration dependence. The only difference between the two theories in describing the molecular weight dependence is that the Doi–Edwards theory defines $D_s \propto M^{-2}$ only for fully entangled solutions, while scaling theory suggests this power law should hold for solutions at concentrations above c^*. Clearly, our data are consistent with M^{-2} at concentrations above c^* as are others.[15,24,25] This indicates that the presence of entanglements is not necessary for establishing reptation as the dominant translational motion within the context of these theories, provided the M^{-2} dependence is a stringent criterion for the reptation mechanism. Of the solution measurements to date, only Amis and Han[24] show significant deviations from the −2 exponent, and there is no way to reconcile that difference at this point, beyond the question of the assignment of the slow mode to self-diffusion.

The concentration dependence of the self-diffusion coefficient in the de Gennes scaling theory is explicitly defined for two limiting solution conditions as mentioned above; in a good solvent, $D_s \propto c^{-1.75}$, and in a Θ-solvent, $D_s \propto c^{-3.0}$. Therefore, a comparison is easily made with our data. Examining the data, as plotted in either Figure 5A or Figure 6, reveals that a unique power law does not exist for the concentration dependence over a wide range in concentration, and the concentration profile is probably best represented as a smooth curve such as the one drawn through the data in Figure 5A. However, scaling theory is successful in certain aspects. Knowing that the pure polymer is a Θ-condition, the good solvent behavior predicted by de Gennes is not expected to hold at large polymer concentrations as noted by Callaghan and Pinder.[23] This implies that $c^{-1.75}$ should best fit the data at concentrations just above c^* for the highest molecular weights and therefore the lowest polymer mass concentrations. We find that to be the case with our data, and that slope is only slowly varying up to about $c = 0.10$ g/g.

As the mass concentration increases, the solution properties should approach Θ-like behavior, as has been shown in static measurements by Daoud et al.[42] Graessley[43] predicted that the crossover should take place in the range from $c = 0.05$ to $c = 0.20$ based on dynamic measurements. As seen in Figure 6, the $c^{-1.75}$ and c^{-3} tangents to the profile intersect within this range. There is no basis for finding steeper slopes in scaling theory, but the theory should not be called upon to account for the tremendous

change that the friction coefficient per subunit undergoes as the solution approaches the glassy state.[8] For our room-temperature measurements, concentrations at which the system will vitrify are not far away on the logarithmic scales used in Figures 4, 5A, and 6. Perhaps, in summarizing this comparison, it should be stated that scaling theory fails to predict the full concentration dependence of a real polymer as expected, but the theory is reasonably successful in predicting limiting values starting from rather simple arguments.

As described earlier the concentration dependence of D_s is expressed in Graessley's[7] formulation of the Doi–Edwards theory phenomenologically in terms of the concentration dependence of the zero-shear viscosity, of chains with molecular weight M_c, $\eta_0(M_c)$, but the measured quantity is typically the zero-shear viscosity, η_0, as a function of concentration for some molecular weight not equal to M_c. Rearranging the relationships from the Doi–Edwards theory, Graessley formulated the following relationship between η_0 and D_s:[7]

$$\eta_0 D_s = G_N^\circ \langle R^2 \rangle / 36 \tag{6}$$

and since $G_N^\circ \propto c^2$, we find

$$D_s/c^2 \propto 1/\eta_0 \tag{7}$$

Thus, a plot of log (D_s/c^2) vs. log η_0 should yield a straight line with a slope of −1.0.

We try such a comparison between our data and the η_0 data of Jamieson and Telford[44] for a narrow-distribution polystyrene of weight-average molecular weight $\bar{M}_w$ = 390 000 in THF at 30 °C which spanned the concentration range from 0.024 to 0.205 g/g. We also make the same type of comparison with the η_0 data of Ferry et al.[45] for polystyrene with $\bar{M}_w$ = 370 000 and a dispersity $(\bar{M}_w/\bar{M}_n)$ of 1.95 in xylene at 25 °C over the concentration range from 0.201 to 0.478 g/g. The comparison is made by scaling our D_s values for samples C, D, and E, by the M^{-2} relationship we found earlier, to the molecular weight of the polymer used in the viscosity measurements and interpolating our data when corresponding concentrations did not exist. For the polystyrene of Ferry et al.,[45] we scale to the weight-average molecular weight as being most representative of the η_0 data. For these two comparisons, we find slopes different from −1.0 for the plots of log (D_s/c^2) vs. log η_0, observing a −1.4 slope with Jamieson and Telford's[44] data and a −1.1 slope with the data of Ferry et al.;[45] thus the Doi–Edwards theory cannot explain the concentration dependence for these measurements.

Beuche et al.[46] showed earlier that

$$D_s/c \propto 1/\eta_0 \tag{8}$$

with data from polystyrenes in solution. More recently, Amis et al.[16] applied this test to QLS slow-mode diffusion coefficients for a gelatin system without success, while Chang and Yu[30] found good agreement for the identical system with D_s values from FRS measurements. This relationship is derived from the free-draining model of Rouse theory for nonentangled solutions[8] from the following two relationships:

$$D_s = kT/n\zeta_0 \tag{9}$$

and

$$\eta_0 = \frac{\zeta_0 nc}{36M_0}\left(\frac{\langle R^2 \rangle}{M}\right) \tag{10}$$

where kT has the usual meaning, n is the degree of polymerization, M_0 is the molecular weight of a monomer unit, ζ_0 is the friction coefficient per monomer unit, and

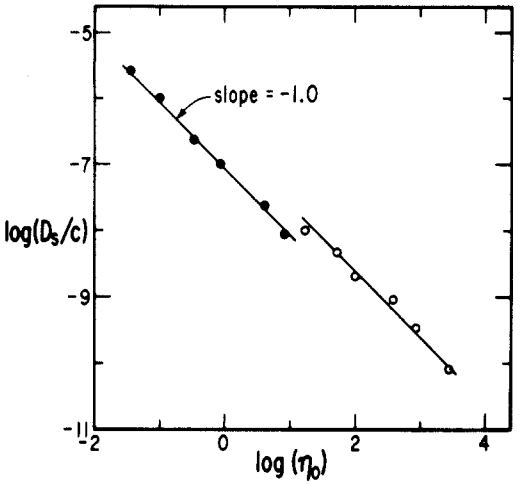

Figure 8. A demonstration of $D_s/c \propto \eta_0^{-1}$ (zero-shear viscosity). Our D_s data combined with η_0 measurements by Jamieson and Telford[44] and Ferry et al.[45] are compared with the prediction of Rouse theory. The filled circles are the η_0 data at corresponding concentrations of Jamieson and Telford[44] for a narrow-distribution polystyrene with $\bar{M}_w$ = 390 000 in tetrahydrofuran at 30 °C and our D_s data for M = 130 000 scaled by M^{-2} to the same molecular weight, 390 000. The unfilled circles are the η_0 data of Ferry et al.[45] for a broader distribution polystyrene ($\bar{M}_w/\bar{M}_n$ = 1.95) for $\bar{M}_w$ = 370 00 in xylene at 25 °C and our D_s data for M = 130 000, and M = 105 000 for $c > 0.30$ g/g, scaled by M^{-2} to M = 370 000, except that the D_s values matching the two largest η_0 data were interpolated with the aid of the plot in Figure 5A. A line with slope −1.0 is drawn through each set of data, indicating good agreement with the Rouse theory. Attempts to scale the η_0 data sets by ratios of solvent viscosities and temperatures fail to bring the data to a single line.

the other parameters are previously defined. When the comparison is now made to the two viscosity data sets, the agreement is excellent as shown in Figure 8. It should be noted that no corrections are applied for the effects of differing solvent viscosities and temperatures, and attempts to scale the viscosity profiles by viscosity and temperature ratios fail to bring all the data to a single line.

The extension of the Doi–Edwards theory, being limited to fully entangled systems, may have failed in this analysis because of the limited number of entanglements in the solutions where the comparison to viscosity data is made, especially noting the better agreement in the higher concentration range. However, the agreement with the Rouse theory prediction is much better over the entire concentration range, and it is therefore a better representation of the data than either molecular model.

One additional comparison with other kinds of data is afforded by using the phenomenological approach used recently by Amis et al.[25] based mainly on works by Graessley.[47] In this description, the diffusion behavior is divided into two distinct zones relative to the concentration for the onset of entanglement behavior, c_e, defined as

$$c_e = M_e^\circ \rho / M \tag{11}$$

where M_e° is the molecular weight between entanglements in the bulk polymer (18 000 for polystyrene[8]) and ρ is the polymer density. At concentrations below c_e, the self-diffusion coefficient is assumed to be described by a freely diffusing Rouse chain by using eq 9. For concentrations above c_e, the motion is characterized by reptation with each blob in a chain described by Rouse chain diffusion but constrained to move along the contour direction of the total chain. This leads to

$$D_s = \frac{kTM_0\rho M_e^\circ}{3M^2 c\zeta_0} \tag{12}$$

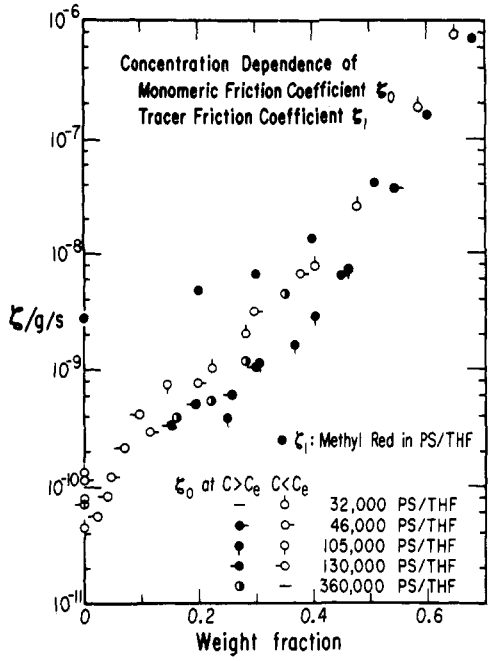

Figure 9. Semilogarithmic plot of the friction coefficients ζ against c. The monomeric friction coefficient ζ_0 calculated by the procedure of Amis et al.[25] and the tracer friction coefficient ζ_1 from the FRS measurements of Landry and Yu[48] for methyl red in polystyrene solutions are both plotted, using the symbols indicated. c_e is the concentration for the onset of entanglement behavior defined in eq 11, and eq 9 and eq 12 show how the nonentangled and entangled ζ_0 values are calculated. The concentration profiles of ζ_0 above and below c_e are shown to differ; that above c_e is slightly lower than that below c_e, reflecting the two-state nature of the model. At high polymer concentrations the ζ_0 and ζ_1 profiles are shown to merge whereas at lower polymer concentrations the two profiles diverge, possibly due to changing hydrodynamic interactions in the polymer coils.

These two relations are used to calculate ζ_0 for each concentration and molecular weight, which can then be compared to data from other experiments, typically viscoelastic measurements, where ζ_0 is most commonly calculated.

We have chosen to compare our self-diffusion data with the tracer diffusion measurements of Landry and Yu[48] for a small molecule, methyl red, diffusing in polystyrene solutions in THF. The friction coefficient of the tracer molecule is calculated by using the Einstein relation

$$D_1 = kT/\zeta_1 \tag{13}$$

and the combined data are shown in Figure 9 in a plot of log ζ vs c. As Amis et al. noted,[25] the ζ_0 values from entangled and nonentangled solutions are grouped in separate but parallel patterns with the entangled values slightly lower over the concentration range measured, probably reflecting the limited two-state nature of the model used. Also, our data, being numerically comparable to that Léger et al.,[15] fall about 1 order of magnitude below the ζ_0's calculated by Amis et al.[25] but follow a parallel trend. The agreement of ζ_0 to ζ_1 is quite good at larger polymer concentrations as expected, but at or near infinite dilution the free dye has a much larger friction coefficient than the corresponding monomer unit, presumably due to changes in the hydrodynamic interactions in the polymer chains. It should also be noted that the Θ-solvent data blend smoothly in this analysis.

In summary, using the FRS technique we have measured the self-diffusion coefficient of dye-labeled polystyrenes at several molecular weights over a much wider range of concentrations than has been done previously. In comparisons of these data to two current molecular models for polymer dynamics, we find that D_s depends on M to the −2 power, in agreement with the Doi–Edwards theory and the de Gennes theory, but neither theory adequately describes the observed concentration dependence. The concentration–viscosity dependence of D_s appears to be best described in terms of a Rouse theory relationship first used by Beuche et al.[46] If the M^{-2} dependence is a stringent requirement to test the reptation model, then the agreement of our data with the Doi–Edwards and de Gennes theories leads us to conclude that reptation is the dominant mode of translation even in solutions without entanglements. We also find that our measurements agree well numerically with those of Léger et al.[15] at low concentrations and that our concentration profiles parallel those observed by Callaghan and Pinder[23] and Amis and Han.[24] Lastly, tracer diffusion measurements[48] are found to be consistent with our self-diffusion coefficient measurements when both are reduced in terms of friction coefficients at larger polymer concentrations.

Acknowledgment. For some 20 years since Hyuk Yu left the laboratory of Professor W. H. Stockmayer at Dartmouth College, he has been scarcely shielded from the impact of his exciting association that was brief in time but has become a lasting fortune. This work is in part supported by a research grant from Eastman Kodak Co. and an NSF grant (Polymers Program, DMR 7908652). We are most grateful to our colleagues, Michael R. Landry for his contributions in refining the FRS apparatus used here, Taihyun Chang for his valuable suggestions for the dye labeling chemistry, and Qi-jiang Gu for his help in the dye synthesis. Thanks are due to Charles Amling for his expert construction of scattering cells. Finally, we thank Professor John D. Ferry and Dr. Eric J. Amis, whose advice and suggestions proved to be invaluable.

Registry No. 4-(Bromomethyl)azobenzene, 57340-21-3; polystyrene (homopolymer), 9003-53-6.

References and Notes

(1) (a) Present address: Research Laboratories, Eastman Kodak Co., Rochester, NY 14650. (b) On leave from the Department of Polymer Science and Technology, Inha University, Incheon 160-01, Korea. (c) On leave from the School of Materials Science, Toyohashi University of Technology, Toyohashi 440, Japan.
(2) Stockmayer, W. H. In "Molecular Fluids"; Balian, R., Weill, G., Eds.; Gordon and Breach: London, 1976; p 108.
(3) Doi, M.; Edwards, S. F. *J. Chem. Soc., Faraday Trans. 2*, **1978**, *74*, 1789, 1802, 1818.
(4) de Gennes, P.-G. *Macromolecules* **1976**, *9*, 587.
(5) de Gennes, P.-G. *Macromolecules* **1976**, *9*, 594.
(6) de Gennes, P.-G. *J. Chem. Phys.* **1971**, *55*, 572.
(7) Graessley, W. W. *J. Polym. Sci., Polym. Phys. Ed.* **1980**, *18*, 27.
(8) Ferry, J. D. "Viscoelastic Properties of Polymers", 3rd ed.; Wiley: New York, 1980.
(9) Bueche, F. *J. Chem. Phys.* **1968**, *48*, 1410.
(10) Klein, J. *Nature (London)* **1978**, *271*, 143.
(11) Klein, J.; Briscoe, B. J. *Proc. R. Soc. London, Ser. A* **1979**, *365*, 53.
(12) Bartels, C. R.; Graessley, W. W.; Crist, B. *J. Polym. Sci., Polym. Lett. Ed.* **1983**, *21*, 495; *Bull. Am. Phys. Soc.* **1983**, *28* (3), 546.
(13) Stejskal, E. O.; Tanner, J. E. *J. Chem. Phys.* **1965**, *42*, 288.
(14) Tanner, J. E. *Macromolecules* **1971**, *4*, 748.
(15) Léger, L.; Hervet, H.; Rondelez, F. *Macromolecules* **1981**, *14*, 1732.
(16) Amis, E. J.; Janmey, P. A.; Ferry, J. D.; Yu, H. *Polym. Bull.* **1981**, *6*, 13; *Macromolecules* **1983**, *16*, 441.
(17) Smith, B. A. *Macromolecules* **1982**, *15*, 469.
(18) Kumagai, Y.; Watanabe, H.; Miyasaka, K.; Hata, T. *J. Chem. Eng. Jpn.* **1979**, *12*, 1.
(19) Kimmich, R.; Bachus, R. *Colloid Polym. Sci.* **1982**, *260*, 911.
(20) Fleischer, G. *Polym. Bull* **1983**, *9*, 152.
(21) Smith, B. A.; Samulski, E. T.; Yu, L.-P.; Winnik, M. A. *Bull. Am. Phys. Soc.* **1983**, *28* (3), 546.

(22) Antonietti, M.; Coutandin, J.; Grütter, R.; Sillescu, H. *Macromolecules* **1984**, *17*, 798.
(23) Callaghan, P. T.; Pinder, D. N. *Macromolecules* **1980**, *13*, 1085; **1981**, *14*, 1334; **1983**, *16*, 968.
(24) Amis, E. J.; Han, C. C. *Polymer* **1982**, *23*, 1403.
(25) Amis, E. J.; Han, C. C.; Matsushita, Y. *Polymer*, in press.
(26) Pohl, D. W.; Schwarz, S. E.; Irniger, V. *Phys. Rev. Lett.* **1973**, *31*, 32.
(27) Hervet, H.; Urbach, W.; Rondelez, F. *J. Chem. Phys.* **1978**, *68*, 2725.
(28) Coutandin, J.; Sillescu, H.; Voelkel, R. *Makromol. Chem., Rapid Commun.* **1982**, *3*, 649.
(29) Brown, G. H., Ed., "Photochromism"; Wiley: New York, 1971.
(30) Chang, T.; Yu, H. *Macromolecules* **1984**, *17*, 115.
(31) Brown, W.; Johnsen, R. M.; Stilbs, P. *Polym. Bull.* **1983**, *9*, 305.
(32) Brandrup, J.; Immergut, E. H., Eds. "Polymer Handbook", 2nd ed.; Wiley: New York, 1975.
(33) Takaki, M.; Asami, R.; Kuwata, Y. *Polym. J.* **1979**, *11*, 425.
(34) Morton, M.; Fetters, L. J.; Inomata, J.; Rubio, D. C.; Young, R. *Rubber Chem. Technol.* **1976**, *49*, 303.
(35) Rubio, D. Ph.D. Thesis, University of Akron, Akron, OH, 1975.
(36) Van Rheenen, V.; Cha, D. Y.; Hartley, W. M. *Org. Synth.* **1978**, *58*, 43.
(37) Burns, J.; McCombie, H.; Scarborough, H. A. *J. Chem. Soc.* **1928**, 2928.
(38) Nanya, H. *Nippon Kagaku Zasshi* **1959**, *80*, 219.
(39) Wesson, J. A.; Takezoe, H.; Yu, H.; Chen, S. P. *J. Appl. Phys.* **1982**, *53*, 6513.
(40) Mandema, W.; Zeldenrust, H. *Polymer* **1977**, *18*, 835.
(41) King, T. A.; Knox, A.; Lee, W. I.; McAdam, J. D. G. *Polymer* **1973**, *14*, 151.
(42) Daoud, M.; Cotton, J. P.; Farnoux, B.; Jannink, G.; Sarma, G.; Benoit, H.; Duplessix, R.; Picot, C.; de Gennes, P.-G. *Macromolecules* **1975**, *8*, 804.
(43) Graessley, W. W. *Polymer* **1980**, *21*, 258.
(44) Jamieson, A. M.; Telford, D. *Macromolecules* **1982**, *15*, 1329.
(45) Ferry, J. D.; Grandine, L. D., Jr.; Udy, D. C. *J. Colloid Sci.* **1953**, *8*, 529.
(46) Beuche, F.; Cashin, W. M.; Debye, P. *J. Chem. Phys.* **1952**, *20*, 1956.
(47) Graessley, W. W. *Adv. Polym. Sci.* **1974**, *16*, 1; **1982**, *47*, 67.
(48) Landry, M. R.; Yu, H., unpublished results.

New Fluorescence Technique for Characterizing Polymer Self-Diffusion†

Thomas Ying-Jung Shiah[1] and Herbert Morawetz*

Department of Chemistry, Polytechnic Institute of New York, Brooklyn, New York 11201.
Received May 23, 1983

ABSTRACT: Dilute solutions of a mixture of naphthalene donor and pyrene acceptor labeled polymers were freeze-dried so that the chain molecules collapsed into globular particles. Pellets pressed from this material were heated above the glass transition temperature, and the emission spectrum was followed as a function of heating time. The interdiffusion of the polymer led to an increase in the nonradiative energy transfer. Data are presented for three molecular weights of polydisperse poly(ethyl methacrylate) and one molecular weight of poly(methyl methacrylate). The method is believed to allow studies of self-diffusion rates smaller than those that can be investigated by other methods.

Introduction

The theoretical analysis of self-diffusion of long flexible-chain molecules by de Gennes[2] and by Doi and Edwards[3] has stimulated a number of workers to devise methods allowing experimental testing of theoretical predictions. Klein and Briscoe[4] followed the diffusion of deuterated polyethylene into normal polyethylene by infrared spectroscopy, and their results confirmed de Gennes' prediction that the self-diffusion coefficient D should be inversely proportional to the square of the chain length. On the other hand, Gilmore et al.,[5] who followed the diffusion of poly(vinyl chloride) into caprolactone by a combination of scanning electron microscopy and energy-dispersive X-ray analysis, found D to vary inversely as the first power of the molecular weight.

Since the dependence of the mean square diffusion distance in a specified direction $\overline{x^2}$ on time, t, is given by $\overline{x^2} = 2Dt$, the ability to measure the very small diffusion coefficients of high polymers depends critically on the spatial resolution of the analytical technique employed. In the method of Klein and Briscoe this resolution was on the order of 10^{-2} cm, allowing estimates of D down to 7×10^{-10} cm^2-s^{-1}, i.e., those of polyethylene with $\overline{M}_w = 23\,000$ at 176 °C. Gilmore et al. were able to estimate D on the order of 10^{-15} cm^2-s^{-1}. In an ingenious method suggested by Sillescu and Zimmer,[6] polystyrene deuterated in the main chain only was to be precipitated, the particles were to be imbedded in perdeuterated polystyrene and the diffusion was to be followed by an NMR technique. With particles having a diameter of 10^{-5} cm (isolated by size fractionation), this technique was expected to allow measurements of D on the order of 10^{-16} cm^2-s^{-1}. Recently, Smith[7] has described the application of fluorescence redistribution measurement after photobleaching for the study of the diffusion at 25 °C of a dye of low molecular weight in poly(methyl methacrylate) containing 18% residual solvent characterized by $D = 1.6 \times 10^{-13}$ cm^2-s^{-1}. The same technique has been used to study the self-diffusion of polymers.[8]

We have used a principle similar to that suggested by Sillescu and Zimmer but which employs a different analytical technique and allows, we believe, even smaller diffusion coefficients to be studied. It has long been known[9] that on freeze-drying dilute solutions of polymers that are glassy at ambient temperatures the individual polymer chains collapse into spherical globules. In a previous study from this laboratory[10] it was shown that if part of the polymer is labeled with a fluorophore (the "donor") whose emission spectrum overlaps the absorption spectrum of a fluorophore (the "acceptor") carried by a second portion of the polymer solute, the fluorescence of the freeze-dried material reflects the original solution concentration, i.e., the extent of the interpenetration of the chain molecules. Thus, when a mixture of donor and

† Dedicated with affection and admiration to W. H. Stockmayer on his 70th birthday.

0024-9297/84/2217-0792$01.50/0